

PRECISE NUCLEOSYNTHESIS LIMITS ON NEUTRINO MASSES

Kimmo Kainulainen

CERN, CH-1211, Geneva 23, Switzerland

A computation of nucleosynthesis bounds on the masses of long-lived Dirac and Majorana neutrinos¹ is reviewed. In particular an explicit treatment of the “differential heating” of the ν_e and $\bar{\nu}_e$ ensembles due to the residual out-of-equilibrium annihilations of decoupled heavy neutrinos is included. The effect is found to be considerably weaker than originally reported by Dolgov et al.². For example, the bounds for a Dirac tau neutrino are $m_{\nu_\tau} < 0.37$ MeV or $m_{\nu_\tau} > 25$ MeV (for $\Delta N_\nu > 1$), whereas the present laboratory bound is $m_{\nu_\tau} < 23.1$ MeV³.

1 Introduction

Nucleosynthesis considerations have proved to be an effective tool in finding limits on particle properties such as masses, couplings, lifetimes, neutrino mixing parameters and so on. The constraining power of nucleosynthesis sensitively depends on the constraints on primordial light element abundances that must be inferred from the observational evidence. This is the difficult part of NS considerations (see K.A. Olive, these proceedings). Nevertheless, as far as NS bounds on new physics are concerned, these details can be summarized by a single parameter: the number of equivalent neutrino degrees of freedom ΔN_ν . The theoretical prediction for the helium abundance on the other hand, with or without new physics, is relatively straightforward and can usually be done very accurately. Parametrizing the deviation of the prediction from the standard result in units of ΔN_ν , one obtains a mapping of the nucleosynthesis bound on the space of parameters of the model. This is the situation in particular for long-lived massive neutrinos, and this is what I mean with “precise” nucleosynthesis bounds.

Massive annihilating particles affect the helium abundance indirectly by altering the expansion rate, or by directly altering the rate of reactions holding neutrons and protons in equilibrium:

$$n + \nu_e \leftrightarrow p + e^- \qquad n + e^+ \leftrightarrow p + \bar{\nu}_e, \qquad (1)$$

during the time $T_\gamma \simeq 0.7$ MeV when the n/p ratio is freezing out. Also, the changes in the expansion rate alter the time available for the free neutron decay $n \rightarrow p + e + \bar{\nu}_e$.

For example, additional mass density speeds up the expansion rate relative to reactions (1), which causes the n/p ratio to freeze out earlier, leaving behind

more neutrons and hence eventually more helium than in the reference case of 3 massless neutrinos. Secondly, since $\mathcal{O}(few)$ MeV neutrinos freeze out at rather low temperatures, their annihilations to $\nu_e \bar{\nu}_e$ final states at temperatures below the *chemical* freeze-out temperature of ν_e 's ($T_{\text{chem}} \simeq 2.3$ MeV) can produce some excess in the ν_e and $\bar{\nu}_e$ number densities (“bulk heating”), leading to an increase of the overall rate of eqs. (1). As a result equilibrium is maintained longer, leading to *less* neutrons and eventually less helium being produced. In section 2 I will review a computation that accurately accounts for these two effects.

Moreover, the residual annihilations of already decoupled heavy neutrinos below $T_{\text{kin}} \simeq 1$ MeV, when ν_e 's fall from *kinetic* equilibrium, can cause a deviation from equilibrium in the tail of the ν_e and $\bar{\nu}_e$ spectra². Although small in amplitude, the effect of these neutrinos is boosted by the quadratic dependence on energy of reactions (1); the detailed balance argument relating the *equilibrium* conversion rates $n \rightarrow p$ and $p \rightarrow n$ does not apply, and simply because there are more protons than neutrons around, the presence of this distortion has the tendency of *increasing* the relative number of neutrons and, eventually, the final helium abundance. I will compute the contribution to ΔN_ν from this “differential heating” in section 3. All effects will be included in the final results, to be presented in section 4.

2 Elements of the Computation

The relevant momentum-dependent Boltzmann equations for the scalar phase-space distribution functions have the form:

$$E_i(\partial_t - pH\partial_p)f_i(p, t) = C_{E,i}(p, t) + C_{I,i}(p, t), \quad (2)$$

where $E_i = (p^2 + m_i^2)^{1/2}$ and $H = (8\pi\rho/3M_{\text{Pl}}^2)^{1/2}$ is the Hubble expansion rate (with M_{Pl} the Planck mass and ρ the total energy density). The index i runs over all particle species in the plasma; each distribution function of each species has an equation like (2), and all of them are coupled through the elastic and inelastic collision terms $C_E(p, t)$ and $C_I(p, t)$.

Since the elastic scattering rates are much higher than the annihilation rates, neutrinos freeze out from the chemical equilibrium remaining in good kinetic contact with the other particles in the plasma. Their spectra can then be described to a very good accuracy by the pseudo-chemical potentials $z_i(T)$, i.e. ($E_i \equiv \sqrt{p^2 + m_i^2}$)

$$f(p, z_i) \equiv (e^{E_i/T_\nu + z_i} + 1)^{-1}; \quad T_\nu \equiv \left(\frac{4 + 2h_e(T_\gamma)}{11} \right)^{1/3} T_\gamma, \quad (3)$$

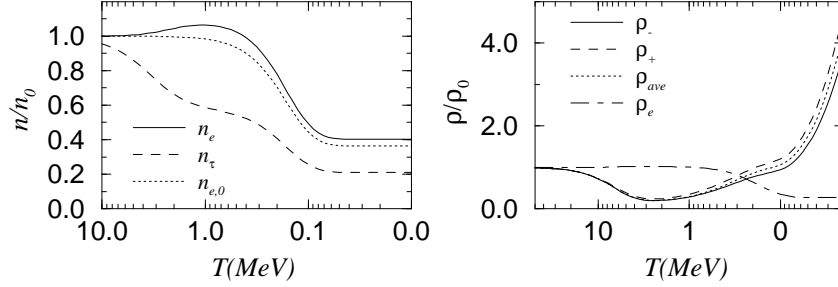


Figure 1: 1a) Electron and tau neutrino number densities with a Majorana ν_τ with $m_{\nu_\tau} = 5$ MeV, normalized to equilibrium density $n_0 \equiv (3\zeta(3)/2\pi^2)T_\gamma^3$. The dashed line for comparison shows the unperturbed electron neutrino temperature. 1b) Energy densities of $\nu_{\tau-}$, $\nu_{\tau+}$ and ν_e with a Dirac ν_τ with $m_{\nu_\tau} = 20$ MeV, normalized to $\rho_0 = 7\pi^2 T_\gamma^4/240$. Also shown is the energy density corresponding to ν_τ in the helicity averaged approximation.

where $h_e(T)$ is related to the entropy stored in the electrons and positrons: $s_e \equiv 2\pi^2 h_e T^3/45$. With the introduction of pseudo-chemical potentials the Boltzmann equations (2) can be integrated over the momenta. One then has a set of coupled ordinary differential equations for the pseudo-chemical potentials of each neutrino species and the photon temperature T_γ^1 .

In fig. 1a a particular solution of the equation network with a mass $m_{\nu_\tau}^M = 5$ MeV is shown. The importance of tracking the ν_e density is clearly visible: the number density of ν_e 's remains close to the equilibrium value until $T \simeq 2.3$ MeV, after which it freezes from chemical equilibrium. Since annihilations of ν_τ 's are still occurring at $T \lesssim 2$ MeV, a slight heating of the electron neutrino distributions results. In the units ΔN_ν , the corresponding effect is⁵ $\delta\Delta N_\nu \simeq -3.6\delta n_{\nu_e}$. In this example $\delta n_{\nu_e} \simeq 0.1$ so that one expects to get $\delta\Delta N_\nu \sim -0.4$, in good agreement with the full nucleosynthesis computation¹.

In the Dirac case there is the additional complication of different helicity states having different interaction strengths at high energies: positive helicity states will freeze out earlier with larger relic density (and the negative helicity states later with smaller) than the hypothetical Dirac neutrino with helicity-averaged interaction strength. One sees this effect in fig. 1b, which shows the energy density stored into different helicities. These deviations almost exactly cancel each other in the sum, however, so that the total number density, and hence the induced effect on helium synthesis, is very close to the results found using the helicity-averaged approach. Figure 1b also shows how the relative energy density stored into tau neutrinos sharply increases at small T .

3 Differential Heating

Qualitatively the physics was explained in the introduction; for more details see Dolgov et al.². Since one is considering a very small amplitude effect in the electron neutrino distributions, one can to a good accuracy use the linearized Boltzmann equation for the deviation. Moreover, because the effect is dominated by large energies, it is an excellent approximation to replace the Fermi–Dirac distributions by Boltzmann distributions. Then noting that the l.h.s. of eq. (2) annihilates the equilibrium distribution, and trading the variables (t, p) for $x_\nu \equiv m_{\nu_\tau}/T_\nu$ and $y \equiv p/T_\gamma$, one gets the generic equation for the deviation:

$$Hx_\nu \frac{\partial}{\partial x_\nu} \delta f(x, y) = C_{\text{ann}}(x, y) - C_{\text{el}}(x, y) \delta f(x, y), \quad (4)$$

where $x \equiv m_{\nu_\tau}/T$. The variables x and x_ν are of course simply related; using x_ν allowed succinctly including the effect of entropy release in eq. (4). The annihilation term $C_{\text{ann}}(x, y)$ acts as a source and it is peaked around $y \simeq x$. The term $C_{\text{el}}(x, y)$ represents the restoring force of the elastic scatterings. In magnitude, $C_{\text{el}} \gg C_{\text{ann}}$. Annihilation terms are easily computed, and I find the forms similar to the ones by Dolgov et al.². On the Dirac case, for example

$$C_{\text{ann}}^D \simeq 9.0 \times 10^{-3} m_{\nu_\tau}^3 \frac{n(x)^2 - n_{\text{eq}}(x)^2}{x^4 \sqrt{y}} \times \exp[-(x - y)^2/y] F_D(x, y), \quad (5)$$

where n 's are the number densities normalized as in fig. 1 and $F_D(x, y)$ is a function with the asymptotic value of 1 for $y \rightarrow 0, x \rightarrow \infty$ ². In numerical work I used exact functions, valid for any x and y , but this is not a significant effect. The elastic scattering term is given by ($n_{\text{eq}}(0) \equiv 1$)

$$C_{\text{el}}(x, y) \simeq 0.75 \frac{m^5 y}{x^5} \left(\frac{T_\nu}{T_\gamma} \right)^4 \left(1 + 0.23 n_{\text{eq}}(x_\nu) + 0.54 \left(\frac{T_\gamma}{T_\nu} \right)^4 n_{\text{eq}}(m_e/T_\gamma) \right). \quad (6)$$

The solution of (4) is straightforward:

$$\delta f(x, y) = \int_0^x dx' A(x') C_{\text{ann}}(x', y) \exp \left[- \int_{x'}^x dx'' A(x'') C_{\text{el}}(x'', y) \right], \quad (7)$$

where

$$A(x) \equiv \frac{1}{x H(x)} \frac{T_\gamma}{T_\nu} \left(1 + \frac{T_\gamma}{3 h_I} \frac{dh_I}{dT_\gamma} \right), \quad (8)$$

and $h_I(T_\gamma) = 2 + h_e(T_\gamma)$. Equations (4) and (7) differ from those of Dolgov et al.² in that I included the dilution due to the entropy release in the electron

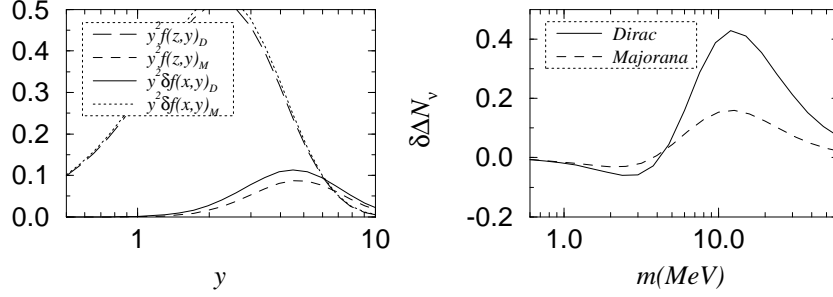


Figure 2: a) The distributions $y^2 \delta f(x, y)$ for $m_{\nu_\tau} = 10$ MeV, and $T = 1$ MeV ($x = 10$) are shown with the corresponding bulk-equilibrium distributions. b) The effect on BBN of the differential heating in units of equivalent ν degrees of freedom.

annihilations, as well as the correct energy dependence in the expansion rate H , both of which tend to weaken the effect. Moreover, the elastic scattering term (6) is somewhat larger than that of Dolgov et al., which also weakens the effect. Fig. 2a displays a particular solution of equation (7) and final results for the effect of differential heating are shown in figure 2b. The effect is largest for the Dirac neutrino at around $m_{\nu_\tau} \simeq 10$ MeV. However, for $m_{\nu_\tau} = 25$ MeV it is already below 0.25 effective neutrino degrees of freedom, i.e. a fourth of that found by Dolgov et al. These results are in very good agreement with the full numerical solution of the Boltzmann equation by Hannestad and Madsen⁶ in the Majorana case.

4 Results

The mass bounds can be expressed in terms of fit functions of ΔN_ν . Including all the effects to the electron neutrino distributions discussed above, we find that the Majorana masses are bounded by

$$\begin{aligned}
 m_\nu^M &< \sqrt{x}(0.350 + 0.047\sqrt{x} + 0.591x) \theta(0.15 - x) \\
 &+ (0.079 + 0.576x + 0.598x^2 - 0.514x^3 + 0.211x^4) \theta(x - 0.15) \\
 m_\nu^M &> 68.59 - 63.83x + 49.18x^2 - 33.09x^3 + 13.18x^4 - 2.17x^5, \quad (9)
 \end{aligned}$$

where the units are MeV and I used $x \equiv \Delta N_\nu$. One sees that opening up a window for a stable tau neutrino below the laboratory bound of 23.1 MeV³ would require relaxing the nucleosynthesis bound to $\Delta N_\nu > 1.44$. Then the NS bound of $\Delta N_\nu < 1$, together with the above laboratory bound rules out a long-lived Majorana tau neutrino with $m_{\nu_\tau}^M > 0.95$ MeV.

In the Dirac case the upper bound on the disallowed region leads to the constraint

$$m_{\nu_\tau}^D > 41.88 - 28.47x + 20.44x^2 - 13.60x^3 + 5.49x^4 - 0.90x^5, \quad (10)$$

where the units are again MeV. The effect of differential heating was for $\Delta N_\nu > 1$ to increase the bound from 22 MeV to $m_{\nu_\tau} > 25$ MeV, closing the window below the experimental bound of $m_{\nu_\tau} < 23.1$ MeV at 95% CL.

The computation of the lower bound on the disallowed region is entirely different from that in the preceding cases and completely unchanged by the differential heating effects. I will only quote the results from Fields et al.: for the bound $\Delta N_\nu > 1$ they give $m_{\nu_\mu} \lesssim 0.31$ MeV and $m_{\nu_\tau} \lesssim 0.37$ MeV, with $T_{QCD} = 100$ MeV. These constraints are conservative in the sense that they would be somewhat stricter if the QCD transition temperature was chosen higher¹.

In conclusion, even with the weak constraint of $\Delta N_\nu < 1$, nucleosynthesis bound is strong enough to exclude a long-lived ($\tau \gtrsim 100$ sec) Majorana tau neutrino with $m_{\nu_\tau} > 0.95$ MeV and a Dirac tau neutrino with $m_{\nu_\tau} > 0.37$ MeV.

Acknowledgements

I wish to thank Sacha Dolgov, Sten Hannestad and Jes Madsen for useful discussions during the Neutrino 96 conference in Helsinki.

References

1. B.D. Fields, K. Kainulainen and K.A. Olive, hep-ph 9512321, CERN-TH/95-335, *Astroparticle Physics* (in press).
2. A.D. Dolgov, S. Pastor and J.W.F. Valle, hep-ph/9602233.
3. ALEPH collaboration, *Phys. Lett. B* **349**, 585 (1995); for the update to 23.1 MeV, see A. Gregorio, these proceedings.
4. K. Enqvist, K. Kainulainen and V. Semikoz, *Nucl. Phys. B* **374**, 392 (1992).
5. K. Enqvist, K. Kainulainen and M. Thomson, *Nucl. Phys. B* **373**, 498 (1992).
6. S. Hannestad and J. Madsen, *Phys. Rev. Lett.* **76**, 2848 (1996); *erratum* hep-ph/9606452.